

Strongly enhanced paramagnetism in $\text{CeNi}_{5-x}\text{Ga}_x$ and LaNi_3Ga_2

J. Tang and L. Li

Department of Physics, University of New Orleans, New Orleans, LA 70148 (USA)

C.J. O'Connor and Y.S. Lee

Department of Chemistry, University of New Orleans, New Orleans, LA 70148 (USA)

Abstract

Low temperature magnetic properties of $\text{CeNi}_{5-x}\text{Ga}_x$ ($x=1, 2, 2.2$ and 2.8) and LaNi_3Ga_2 were investigated. $\text{CeNi}_{5-x}\text{Ga}_x$ show low temperature behaviors that are characteristic of strongly enhanced paramagnetic 3d metals. Gallium additions tend to bring the systems closer to the paramagnetic-itinerant ferromagnetic transition. The valence state of cerium remains at nearly 4+ throughout the series. LaNi_3Ga_2 shows T^2 dependence in both its low temperature resistivity and susceptibility. This implies that the material is a spin fluctuator which possesses a positive curvature in the density of states at the Fermi level.

1. Introduction

CeNi_5 is paramagnetic down to the lowest temperature measured. Its magnetic susceptibility $\chi(T)$ does not follow the Curie–Weiss behavior but shows a broad maximum at about 100 K. The first interpretation for this behavior was that CeNi_5 is in an intermediate valence state and the maximum in $\chi(T)$ results from an increase in the valence state of cerium from 3+ as temperature is decreased [1]. Later studies indicated, however, that cerium is non-magnetic and nearly in the 4+ state at all temperatures [2–5]. The maximum in $\chi(T)$ originates from the 3d electrons of nickel atoms instead of 4f electrons of cerium. This susceptibility maximum comes from a thermal smearing of the density of states at the Fermi level enhanced by spin fluctuations. Such a behavior is possible when the density of states at the Fermi level has a positive curvature due to 3d–5d hybridization [6].

The relative positions of the Fermi levels of nickel and cerium metals are such that 5d electrons of cerium will transfer to the 3d band of nickel when they are combined to form intermetallic compounds. This electron transfer results in a Fermi level that lies in the hybridized band of 3d and 5d electrons, and its position relative to that of 4f level is highly dependent upon the cerium or nickel content. When it is nickel rich, which is the case in CeNi_5 , the Fermi energy is lower than the 4f level. The 4f electrons thus transfer to the hybridized d band leading to an almost empty 4f level, and cerium is in nearly 4+ state. This is the reason why magnetism in CeNi_5 arises from d electrons (mainly

3d electrons). As nickel content decreases (cerium content increases), the Fermi energy increases until it rises above the 4f level. The 4f states are filled under such conditions and cerium has a localized magnetic moment and is in 3+ valence state. An example of cerium rich compounds exhibiting local moments is Ce_7Ni_3 . It orders antiferromagnetically at 1.8 K and its cerium atoms have a valence close to 3+ [6]. There is also an indication that Ce_7Ni_3 is a Kondo lattice from its low temperature resistivity measurement. Between these two extremes, *i.e.* when the cerium or nickel contents are intermediate, the Ce–Ni system exhibits intermediate valence behavior as found in CeNi [7].

Studies on other Ce–Ni and related systems have also indicated a similar correlation between the nickel content and valence state of cerium. A systematic study on $\text{Ce}(\text{Cu}_{1-x}\text{Ni}_x)_5$ revealed that the cerium undergoes a transition from trivalent to quadrivalent states as x increases from 0 to 1 [5]. The change in the position of the 4f level relative to the Fermi level when x was varied resulted in the following sequence of transitions: from a magnetic 4f metal ($T_N=3.8$ K) ($0 < x < 0.1$) to a non-magnetic Kondo lattice ($0.1 < x < 0.5$), and then to a mixed valence compound ($0.5 < x < 0.9$), and finally to a non-magnetic 3d metal ($x=1$). Koterlin *et al.* [8] reported an investigation on compounds of CeNiGa_y ($y=0.5, 2$ and 3). Their study suggested that, as y was decreased from 2 to 0.5 and therefore the relative nickel content in the compounds was increased, the system changed from a Kondo lattice to a mixed valence state. Another series $\text{CeNi}_x\text{Ga}_{4-x}$ ($x=0.5$ – 1.1) exhibits

a transition from weakly ferromagnetic at the gallium rich side to non-magnetic at the nickel rich side [9], which suggests that increasing nickel content suppresses magnetic ordering.

In this paper, we report our investigation on the low temperature properties of $CeNi_{5-x}Ga_x$ ($x = 1, 2, 2.2$ and 2.8). Our study was also motivated by the heavy fermion behavior found in the structurally related compounds UNi_2Al_3 [10] and by the controversies surrounding the heavy fermion behavior of $CeCu_3Al_2$ and $CeCu_4Ga$ which have the same crystal structure as $CeNi_5$ [11].

2. Experimental details

Samples of $CeNi_{5-x}Ga_x$ ($x = 0, 1, 2, 2.2$ and 2.8) and $LaNi_3Ga_2$ were prepared by melting the constituents in an arc furnace under an argon atmosphere. The starting metals used were purchased from Aldrich Chemical Company and had purity levels of 3N, 3N5 and 5N for cerium, nickel and gallium, respectively. All as-cast samples, except for $CeNi_{2.2}Ga_{2.8}$, showed no trace of any second phase in their optical micrographs. $CeNi_{2.2}Ga_{2.8}$ contained a small amount of second phase(s), a portion of which still remained after a heat treatment at 600 °C for 10 days. The X-ray diffraction pattern of the as-cast $CeNi_{2.2}Ga_{2.8}$ sample contained peaks from the impurity phase(s), and they disappeared from the X-ray pattern after the heat treatment. X-Ray diffraction is normally less sensitive to an impurity phase than optical microscopy and might not have detected the small amount of impurities present in the heat treated sample.

Crystal structures and lattice parameters of $CeNi_{5-x}Ga_x$ were determined from X-ray diffraction experiments conducted on a SCINTAG X-ray powder diffractometer. $CeNi_5$ and $CeNi_4Ga$ ($x = 0$ and 1) were found to crystallize in the $CaCu_5$ -type hexagonal structure. $CeNi_3Ga_2$, $CeNi_{2.8}Ga_{2.2}$ and $CeNi_{2.2}Ga_{2.8}$ ($x = 2, 2.2$ and 2.8) crystallize in the $HoNi_{2.6}Ga_{2.4}$ -type hexagonal structure. Their lattice parameters are listed in Table 1. The phase diagram of Ce–Ni–Ga ternary system has been studied by Gryn [12]. He found that $CeNi_{5-x}Ga_x$ ($x = 0–1.6$) has the $CaCu_5$ -type structure and, for $x = 2–2.2$, it has the $HoNi_{2.6}Ga_{2.4}$ -type structure. As x further increases, it comes back to the $CaCu_5$ -type structure at $x = 2.8$. It does not exist for composition with $x > 2.8$. Our results are consistent with those of Gryn for $x = 0, 1, 2$ and 2.2 . However, for $x = 2.8$, different structures were reported. This discrepancy needs to be further examined. It should be mentioned that the exact composition of our $x = 2.8$ sample may not be $CeNi_{2.2}Ga_{2.8}$ since an impurity phase(s) was present in the sample.

TABLE 1. Lattice parameters and unit cell volumes of $CeNi_{5-x}Ga_x$ and $LaNi_3Ga_2$ determined from this study

Compound	a (Å)	c (Å)	v (Å ³)
$CaCu_5$ -type			
$x = 0$	4.880	4.013	82.76
$x = 1$	4.966	4.072	86.97
$HoNi_{2.6}Ga_{2.4}$ -type			
$x = 2$	8.861	4.096	278.5
$x = 2.2$	8.892	4.086	279.8
$x = 2.8$	9.064	4.073	289.8
$LaNi_3Ga_2$	9.070	4.105	292.5

As seen in Table 1, lattice parameter a increases as gallium concentration increases in both types of structures. This is because the metallic radius of gallium is larger than that of nickel. Lattice parameter c increases with gallium concentration in the $CaCu_5$ -type structure and decreases slightly in the $HoNi_{2.6}Ga_{2.4}$ -type structure. Although c decreases with gallium content in the latter case, the overall unit cell volume still increases as gallium content is increased. One interesting point to mention is that c does not change much between the two different types of structures. Since c is also the smallest spacing between two cerium atoms in a unit cell, one may speculate that the physical properties corresponding to the 4f electrons of cerium might not be significantly different.

$LaNi_3Ga_2$ has the same crystal structure as $CeNi_3Ga_2$ and its lattice parameters a and c are both larger than those of $CeNi_3Ga_2$ (see Table 1). As seen, the increase in a due to the replacement of cerium by lanthanum is much more significant than the increase in c . In fact, a increases by more than 2% but c increases only 0.2%. c is also less affected by gallium substitution than a in the $HoNi_{2.6}Ga_{2.4}$ -type structure where a increases by more than 2% and c decreases by only about 0.5% when x is increased from 2 to 2.8.

Low temperature DC magnetic susceptibility χ was measured for $CeNi_{5-x}Ga_x$ ($x = 1, 2, 2.2$ and 2.8) and $LaNi_3Ga_2$ using a SQUID susceptometer from 2 to 300 K. The applied measuring field was 250 G. DC resistivity measurements were conducted on $CeNi_3Ga_2$ and $LaNi_3Ga_2$ in a closed cycle helium refrigerator using a four-point technique.

3. Results and discussion

Shown in Fig. 1 is the susceptibility versus temperature plot for $CeNi_5$ and $CeNi_4Ga$. Data on $CeNi_5$ were extracted from ref. 5. The broad maximum around 100 K in the χ of $CeNi_5$ is apparent. If one disregards, for the sake of discussion, the low temperature tail in

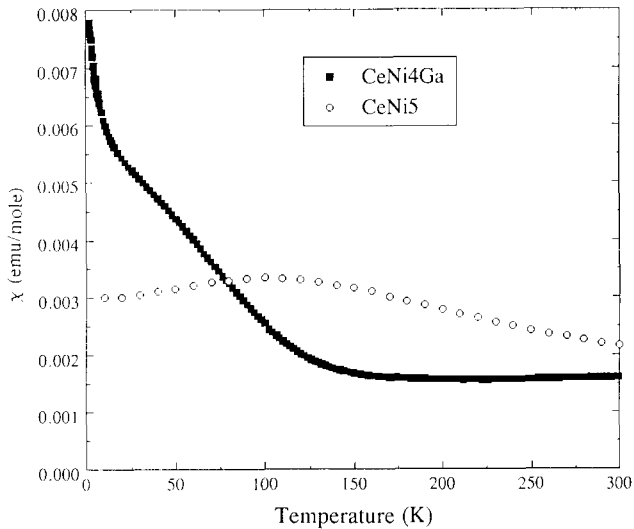


Fig. 1. Susceptibility χ versus temperature T of $CeNi_5$ and $CeNi_4Ga$. Data on $CeNi_5$ were extracted from ref. 5.

the susceptibility, this maximum also exists in $CeNi_4Ga$ and is shifted to a lower temperature. The maxima in χ arise from the thermal smearing of the hybridized 3d density of states at the Fermi level enhanced by spin fluctuation. According to the band and paramagnon theories [13], T_{max} , the temperature where $\chi(T)$ reaches maximum, has no special physical meaning in itself. The maximum is the result of the competition between the increasing χ at low temperatures and decreasing χ at high temperatures. Nevertheless, Sakakibara *et al.* [14] found a correlation between T_{max} and the critical field of the metamagnetic transition in $M(Co_{1-x}Al_x)_2$ ($M = Y$ and Lu). Their study suggested that the smaller the T_{max} , the closer the system is to the ferromagnetic state. Taking this statement as valid for $CeNi_{5-x}Ga_x$ one finds that gallium addition to $CeNi_5$ favors the itinerant ferromagnetic ground state. The low temperature tail in the susceptibility of $CeNi_4Ga$ is another indication that the system is about to order ferromagnetically. The tail could also arise from magnetic impurities. Assuming that the impurity is Ce^{3+} and it has an effective moment equal to the Hund's rule value of $2.54 \mu_B$, we have tried to fit the tail portion of the χ data into a Curie-Weiss law after a constant χ_0 ($\chi_0 = 0.0024$ emu/mol) had been taken out. A Curie constant C of 0.08 emu K/mol determined from the fit implies that 10% of cerium in the sample would have been in the impurity state. This is rather unlikely since the optical micrograph showed an impurity-free uniform sample. We are inclined to believe that the tail is intrinsic and $CeNi_4Ga$ is near the transition to an itinerant ferromagnetic metal. Further measurements on magnetization and hysteresis will be helpful in confirming this interpretation. Such experiments are being planned.

Figure 2 shows the χ versus T curves of $LaNi_3Ga_2$, $CeNi_3Ga_2$, $CeNi_{2.8}Ga_{2.2}$ and $CeNi_{2.2}Ga_{2.8}$. The χ of $LaNi_3Ga_2$ exhibits a maximum around 25 K which has the same origin as that of $CeNi_5$. Between 10 K and 20 K, $\chi(T)$ increases as T^2 . χ can be well fitted to the equation $\chi(T) = A + BT^2$, with $A = 0.0013$ emu/mol and $B = 1.6 \times 10^{-7}$ emu/mol K². This temperature dependence of χ was predicted from the band and paramagnon theories, and the positive value of B results from the positive curvature of the density of states at the Fermi level due to 3d-5d hybridization [13]. At even lower temperatures, one can see clearly an upturn in χ , which we believe comes from magnetic impurity. Assuming the impurity is Ni^{2+} , a similar fitting procedure to the one described earlier indicated that 0.08% of Ni is in the impurity state. The presence of such a tiny amount of Ni^{2+} impurity in the sample is very likely.

The susceptibilities of $CeNi_3Ga_2$ and $CeNi_{2.8}Ga_{2.2}$ are similar and show no special feature except the low temperature tails. Whether the tails are intrinsic or extrinsic is unclear. If they are extrinsic, the Curie-Weiss law fits to the tail portions of the χ set an upper limit of the impurity level of 0.5%. A detailed examination reveals that these susceptibilities increase with temperature above 100 K. This indicates that χ may develop a maximum above room temperature in these two compounds. It is known that the differences in the behavior of cerium and lanthanum compounds are normally caused by the 4f electron of cerium atoms. However, the 4f level in $CeNi_3Ga_2$ is almost empty, and this transfer of the 4f electrons to the d band causes only a certain degree of modification of the density of states at the Fermi level. This is the reason why both $CeNi_3Ga_2$ and $LaNi_3Ga_2$ behave like strongly enhanced paramagnetic 3d metals. The difference between the two compounds is due to a change in the density of states at the Fermi level induced by transfer

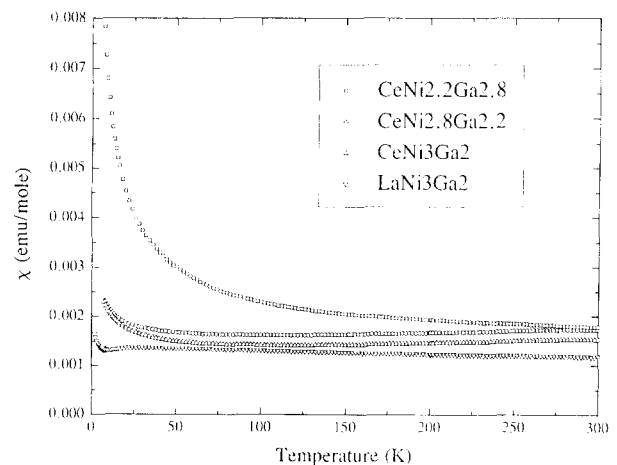


Fig. 2. Susceptibility χ versus temperature T of $LaNi_3Ga_2$, $CeNi_3Ga_2$, $CeNi_{2.8}Ga_{2.2}$ and $CeNi_{2.2}Ga_{2.8}$.

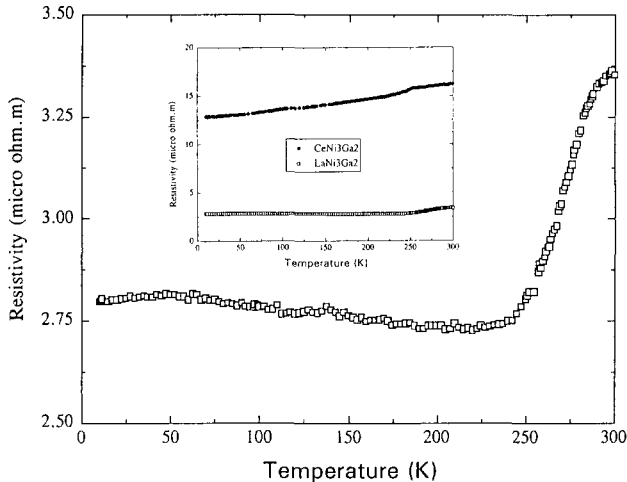


Fig. 3. Resistivity ρ versus temperature T of $LaNi_3Ga_2$; inset: the same plot for both $LaNi_3Ga_2$ and $CeNi_3Ga_2$.

of the 4f electrons to the d band and by changes in the lattice parameters, which affect the hybridization between the bands involved.

In $CeNi_{2.2}Ga_{2.8}$, the high gallium content relative to that in $CeNi_{3-2.8}Ga_{2-2.2}$ leads to a behavior that can be characterized as near the transition between strongly enhanced paramagnetic metal and itinerant ferromagnetic state. This is obviously seen in the enhanced upturn in the $\chi(T)$ of $CeNi_{2.2}Ga_{2.8}$. Neither peak nor saturation has been found in $\chi(T)$ down to the lowest temperature measured. The effect of gallium addition is reminiscent of that found when x was increased from 0 to 1 in $CeNi_{5-x}Ga_x$, i.e. gallium addition brings the systems closer to the ferromagnetic state. On the other hand, this sample contained small amount of impurity phase as mentioned earlier, thus the possibility that the low temperature tail arises from the impurity cannot be ruled out. By fitting the low temperature tail to a Curie-Weiss law, the amount of cerium (assuming Ce^{3+}) present in the impurity phase was estimated to be about 7%.

Resistivity measurements were conducted on $CeNi_3Ga_2$ and $LaNi_3Ga_2$. Figure 3 shows the resistivity ρ versus T plot for $LaNi_3Ga_2$, and the inset shows the combined plot for both. An interesting feature of the $\rho(T)$ of $LaNi_3Ga_2$ is that it has a negative slope between 50 K and 200 K, makes a broad maximum around 50 K and then decreases with decreasing temperature, following a T^2 dependence below 30 K. The low temperature T^2 dependence, which is typical of a Fermi liquid, suggests the importance of spin fluctuation in $LaNi_3Ga_2$. The resistivity data ($T < 30$ K) were fitted to the equation $\rho(T) = \rho_0 + AT^2$, which resulted in $\rho_0 = 2.8 \mu\Omega\text{-m}$ and $A = 1.2 \times 10^{-5} \mu\Omega\text{-m/K}^2$. It is known that the negative slope of $\rho(T)$ is normally associated with the Kondo scattering and found mostly in systems

where local moments exist. The cause for the negative slope in $\rho(T)$ of $LaNi_3Ga_2$, which has no localized moment, is unclear. The resistivity of $CeNi_3Ga_2$ is that of a normal metal. The sudden increase at 250 K is probably due to microcracks developing in the sample during heating.

4. Conclusions

$CeNi_{5-x}Ga_x$ ($x=0, 1, 2, 2.2$ and 2.8) crystallize in two types of structures: $CaCu_5$ -type ($x=0$ and 1) and $HoNi_{2.6}Ga_{2.4}$ -type ($x=2, 2.2$ and 2.8). All samples of both structure types show low temperature behavior that is characteristic of strongly enhanced paramagnetic 3d metals. Gallium additions tend to bring the systems closer to the transition between the paramagnetic state and itinerant ferromagnetic state. However, it was not able to raise the Fermi energy to, or close to, the 4f level and, therefore, the valence state of cerium remained at nearly $4+$ throughout the series. $LaNi_3Ga_2$ shows T^2 dependence in both its low temperature resistivity and susceptibility. This implies that the material is a spin fluctuator which possesses a positive curvature in the density of states at the Fermi level.

References

- 1 K.H.J. Buschow, M. Brouha, H.J. van Daal and H.R. Miedema, in R.D. Parks (ed.), *Valence Instabilities and Related Narrow band Phenomena*, Plenum, New York, 1977, p. 125.
- 2 D. Gignoux, F. Givord, R. Lemaire, H. Launois and F. Sayetat, *J. Phys. (Paris)*, **43** (1982) 173.
- 3 D. Gignoux, F. Givord, R. Lemaire and F. Tasset, *J. Phys. (Paris)*, **43**(C7) (1982) 257.
- 4 S. Cabus, K. Gloos, U. Gottwick, S. Horn, M. Klemm, J. Kübler and F. Steglich, *Solid State Commun.*, **51** (1984) 909.
- 5 N.B. Brandt, V.V. Moschchalkov, N.E. Sluchanko, E.M. Savitskii and T.M. Shkatova, *Sov. Phys. Solid State*, **26** (1984) 1279.
- 6 D. Gignoux and J.C. Gormez-Sal, *J. Appl. Phys.*, **57** (1985) 3125.
- 7 D. Gignoux, F. Givord, R. Lemaire and F. Tasset, *J. Less-Common Met.*, **94** (1983) 165.
- 8 M.D. Koterlin, B.S. Morokhivskii and Yu.M. Grin, *Sov. Phys. Solid State*, **30** (1988) 517.
- 9 E.V. Sampathkumaran and I. Das, *Solid State Commun.*, **81** (1992) 901.
- 10 C. Geibel, S. Thies, D. Kaczorowski, A. Mehner, A. Grauel, B. Seidel, U. Ahlheim, R. Helfrich, K. Petersen, C.D. Bredl and F. Steglich, *Z. Phys. B: Cond. Mat.*, **83** (1991) 305.
- 11 S.K. Dhar and K.A. Gschneidner, Jr., *J. Magn. Magn. Mater.*, **79** (1989) 151.
- 12 Yu.N. Gryn, *Ph.D. Thesis*, Lvov State University, Lvov, Ukraine, 1980, p. 1.
- 13 M.T. Beal-Monod, *Physica B*, **109/110** (1982) 1837.
- 14 T. Sakakibara, T. Goto, K. Yoshimura, K. Murata and K. Fukamichi, *J. Magn. Magn. Mater.*, **90/91** (1990) 131.